

# CCRL2 affects the sensitivity of myelodysplastic syndrome and secondary acute myeloid leukemia cells to azacitidine

Theodoros Karantanos,<sup>1</sup> Patric Teodorescu,<sup>1</sup> Marios Arvanitis,<sup>2</sup> Brandy Perkins,<sup>1</sup> Tania Jain,<sup>1</sup> Amy E. DeZern,<sup>1</sup> W. Brian Dalton,<sup>1</sup> Ilias Christodoulou,<sup>1</sup> Bogdan C. Paun,<sup>1</sup> Ravi Varadhan,<sup>3</sup> Christopher Esteb,<sup>1</sup> Trivikram Rajkhowa,<sup>1</sup> Challice Bonifant,<sup>4,5</sup> Lukasz P. Gondek,<sup>1</sup> Mark J. Levis,<sup>1</sup> Srinivasan Yegnasubramanian,<sup>5</sup> Gabriel Ghiur<sup>1</sup> and Richard J. Jones<sup>1</sup>

<sup>1</sup>Division of Hematological Malignancies, Department of Oncology, Sidney Kimmel Comprehensive Cancer Center; <sup>2</sup>Division of Cardiology, Department of Medicine; <sup>3</sup>Division of Biostatistics and Bioinformatics, Department of Oncology, Sidney Kimmel Comprehensive Cancer Center; <sup>4</sup>Department of Pediatrics and <sup>5</sup>Department of Oncology, Sidney Kimmel Comprehensive Cancer Center, Johns Hopkins University School of Medicine, Baltimore, MD, USA

**Correspondence:** T. Karantanos  
[tkarant1@jhmi.edu](mailto:tkarant1@jhmi.edu)

**Received:** May 24, 2022.

**Accepted:** December 2, 2022.

**Early view:** December 15, 2022.

<https://doi.org/10.3324/haematol.2022.281444>

©2023 Ferrata Storti Foundation

Published under a CC BY-NC license



## **SUPPLEMENTARY METHODS**

### **Cell lines and reagents**

MDS92 and MDS-L cells were a kind gift of Dr. Starczynowski (University of Cincinnati). TF-1 cells were purchased from the American Type Culture Collection (ATCC) (CRL-2003). Chlophosome-A chlodronate liposomes was purchased from FormuMax Scientific (#F70101C-A), doxycycline (doxy) was purchased from Millipore Sigma (#24390-14-5) and azacitidine was purchased from Selleckchem (#S1782) respectively.

### **CCRL2 lentiviral knockdown**

Lentiviral vectors expressing CCRL2-targeting shRNA (RHS3979-201740504 – sh1, RHS39379-201740506 – sh2 and RHS3979-201740505 – sh3) (Horizon), or non-targeting mammalian shRNA pLKO.1-puro lentiviral vector (NTV, Sigma Aldrich) were transfected into HEK-293FT cells. MDS92, MDS-L and TF-1 cells were transduced with lentiviruses and selected with puromycin (2 µg/ml and 1 µg/ml).

### **CD34+ cells collection**

Bone marrow samples were procured from bone marrow aspirations of MDS and MDS/MPN patients before the initiation of disease-modifying therapy. Appropriate informed consent was obtained from all donors in accordance with the Declaration of Helsinki and under a research protocol approved by Johns Hopkins Institutional Review Board. CD34+ cell subsets were isolated using the CD34 MicroBead kit (Miltenyi Biotec).

### **Analysis of raw RNA-seq data**

Raw RNA-seq reads were processed using the ENCODE DCC RNA-seq analysis pipeline. Reads were mapped to the hg38 version of the human genome using the STAR aligner v2.4.2 and reads that overlap exonic regions were aggregated using RSEM v1.2.31 with gencode v29 as reference to produce a counts matrix. DESeq2 was used to normalize the gene expression results using a size factor that accounts for library size and gene size. This was followed by a variance stabilizing transformation as implemented in DESeq2, the output of which was used to perform PCA. Surrogate variable analysis (SVA) was employed to control for confounders and batch effects. Differential expression (DE) was tested based on a negative binomial Wald statistic with a two-tailed alternative hypothesis as implemented in DESeq2, using identified surrogate variables from SVA as covariates. A corresponding p-value was generated from the Wald statistic and adjusted for multiple testing using false discovery rate (FDR). Genes were considered significant if their FDR was  $< 0.05$ . Gene set enrichment analysis was performed using the GSEA package. Each gene's negative binomial Wald statistic as the ranking parameter for GSEA, and the rank list was tested against the curated gene sets available in MSigDB (17). Gene sets were considered significant if their FDR was  $< 0.05$ .

### **Clonogenicity assays**

Cells following treatment were collected, counted, and resuspended at a density of 2000 cells/ml in methylcellulose-based media. After 10 to 14 days of incubation at  $37^{\circ}\text{C}$  in 5%  $\text{CO}_2$ , the recovery of colony-forming units was determined by colony counting under bright-field microscopy. A cell aggregate composed of  $>50$  cells was defined as a colony. For serial passage experiments, colonies were collected at day 14 and cells were re-seeded onto methylcellulose medium at a density of 2000 cells/ $9.6\text{ cm}^2$  and cultured for a further 15 days for formation of clones

in the secondary passage (P2). This process continued for total 3 passages. The azacitidine IC50 concentration was calculated using the CalcuSyn version 2.0 software.

### **CRISPR-Cas9 CCRL2 editing**

Three pre-designed single guide RNAs (sgRNAs) targeting CCRL2 (Hs.Cas9.CCRL2.1.AA – sgRNA1, Hs.Cas9.CCRL2.1.AC – sgRNA2 and Hs.Cas9.CCRL2.1.AF) were purchased from Integrated DNA Technologies (IDT). RNP complexes were prepared by combining 50  $\mu$ M gRNA with 61  $\mu$ M Cas9 nuclease also purchased from IDT (#1081061).  $10^5$  TF-1 cells were suspended in nucleofection buffer purchased from IDT (#11-05-01-05) and mixed with the RNP complex and 100  $\mu$ M Alt-R Cas9 Electroporation Enhance (#1075916) and plated in a 96-well Nucleocuvette module purchased from Lonza (#AAF-1003S). TF-1 cells mixed with Cas9 nuclease alone were used as controls. Electroporation was performed in a 4D-Nucleofector™ Core Unit (DN-100). Subsequently cells were seeded as single cells into 96-well plates. DNA from growing clones was extracted and sequenced using pre-designed primers (Forward 5' – TCATCTCCCATTCTCCACAGG and Reverse 5' – CAAGTGTCCTGGATGGGTAAC) purchased IDT. DNA sequencing was performed by the Synthesis and Sequencing Facility of the Johns Hopkins University. Clones with homozygous deletion, frameshift or nonsense mutations of CCRL2 were analyzed for CCRL2 expression by flow cytometry. The clones with the lowest CCRL2 expression from each sgRNA group were selected for clonogenicity studies.

### **Development of a doxy-induced CCRL2 expression model**

Lentiviral vectors expressing pLV-Puro-TRE-CCRL2 (VB220215-1194ruu) and pLV-Hygro-CMV>tTS/rtTA (VB010000-9369xhm) (VectorBuilder) were transfected together with pCMV-dR8.9 and vesicular stomatitis virus G-expressing plasmids into 293T cells using Lipofectamine

2000 (Thermo Fisher Scientific) for lentiviral supernatant production. MDS-L and TF-1 cells with CCRL2 deletion by CRISPR-Cas9 were incubated with the viral supernatant and polybrene (8 µg/ml; MilliporeSigma) for transduction. Transductions were performed sequentially for the two viruses. After at least 48 hours from each transduction, cells were selected with puromycin (2 µg/ml; Millipore Sigma) for the first transduction and hygromycin (300 µg/ml, Thermo Scientific) for the second transduction. Subsequently, cells were treated with 0, 0.5 and 1 µg/ml doxy and CCRL2 expression was assessed by western blot and flow cytometry.

### **Flow cytometry analysis**

Primary CD34<sup>+</sup> cells were labeled antibodies against CD34 (Fluorescein isothiocyanate (FITC)-conjugated anti-CD34, BD Biosciences, #555821) and 7AAD (BD Biosciences, #559925). Cells were then fixed in 4% formaldehyde for 15 minutes and permeabilized in 100% methanol for 30 minutes. Subsequently, cells were labeled with conjugated antibodies (Phycoerythrin (PE)-conjugated anti-CCRL2, (BioLegend, ) (#358303, PE-cyanine 7 (Cy7)-conjugated anti-CD11b, Biosciences, #557743, PE-conjugated anti-CD14 (BioLegend) (#367103), Alexa-Flour 488-conjugated anti-CD16, BioLegend, #302022, FITC-conjugated anti-CD41, BioLegend, #303703, FITC-conjugated anti-CD41, BioLegend, #303703, PE-conjugated anti-CD61, BioLegend, #336405, PE-Cy7-conjugated anti-CD71 (BioLegend) (#113811), Allophycocyanin (APC)-conjugated anti-CD235a, BioLegend, #349113, Annexin V and PI, BD Biosciences, #556547). Gating was based on clearly distinguishable populations, or in the absence of such, the negative antibody control. For the differentiation analysis cells were not fixed or permeabilized. Stained cells were analyzed using the BD LSR II (BD Biosciences). Median fluorescence intensity (MFI) was determined for each marker using FlowJo analysis software version 10.0.8 (FlowJo, Ashland, CO, USA).

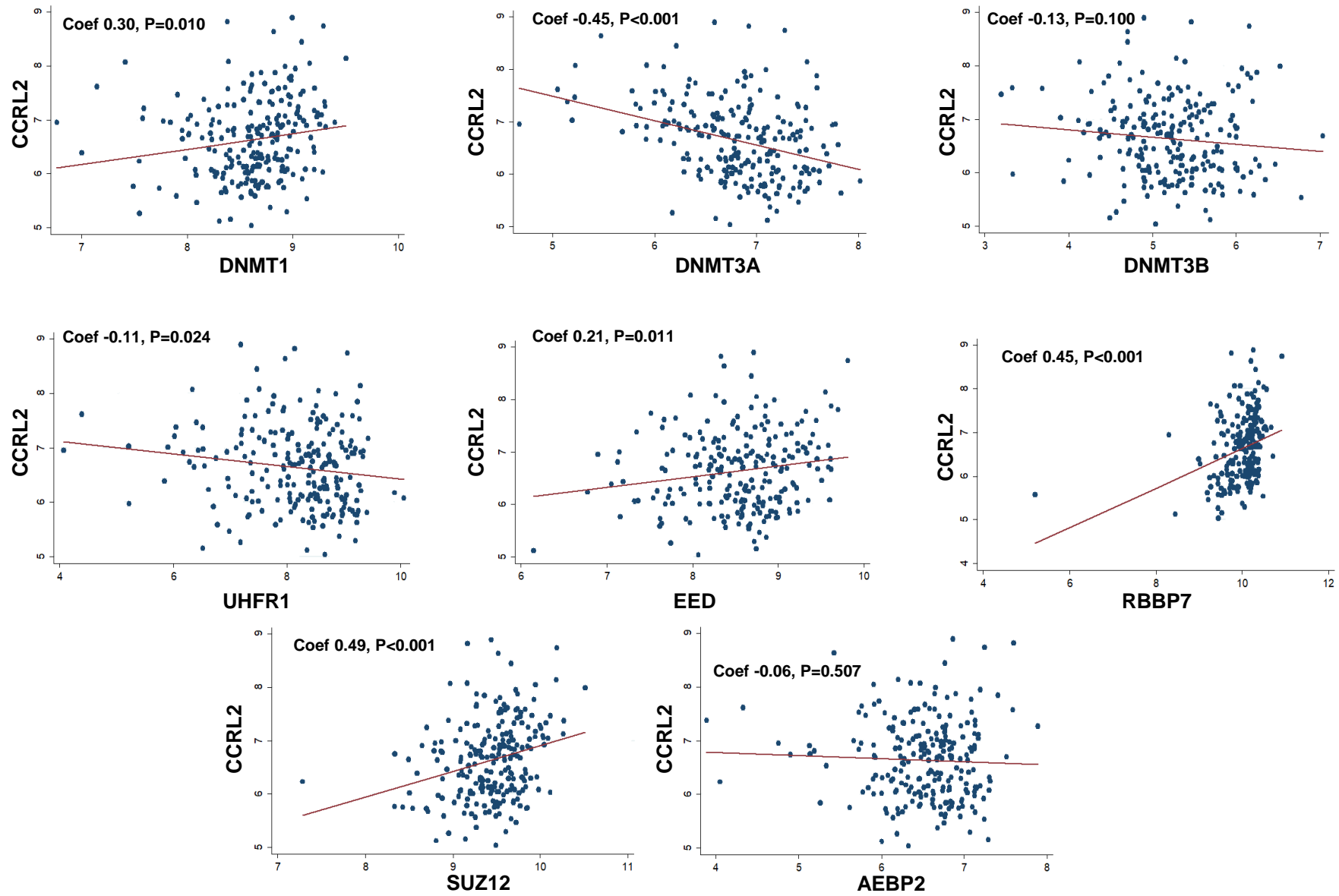
## **Western blotting Antibodies**

- 1) Anti-DNMT1 (Cell Signaling Technology) (#5032)
- 2) Anti-DNMT3A (Cell Signaling Technology) (#3598)
- 3) Anti-DNMT3B (Cell Signaling Technology) (#67259)
- 4) Anti- $\beta$ -actin (Cell Signaling Technology) (#4970)
- 5) Anti-CCRL2 (LSBio) (LS-C382506)
- 6) Anti-p27 (Cell Signaling Technology) (#3686)
- 7) Anti-Phospho-Rb (Ser807/811) (Cell Signaling Technology) #8516
- 8) Anti-Rb (Cell Signaling Technology) (#9302)
- 9) Anti-SUZ12 (Cell Signaling Technology) (#3737)
- 10) Anti-LIN28B (Cell Signaling Technology) (#4196)
- 11) Anti-GNAQ (Abcam) (#210004)
- 12) Anti-E2F1 (Cell Signaling Technology) (#3742)
- 13) Lamin B1 (Cell Signaling Technology) (#12586)

## **Statistical Methods**

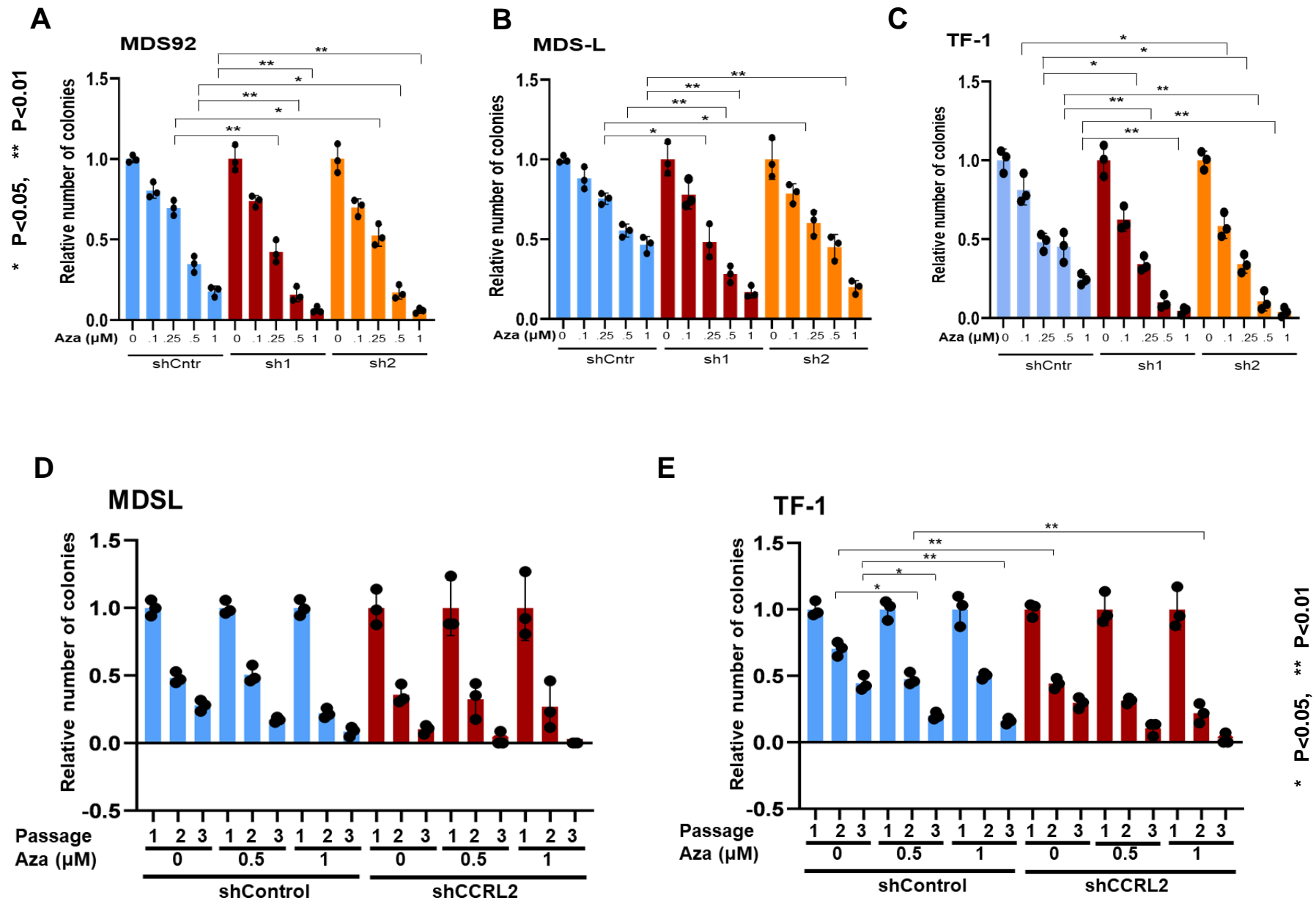
Unpaired 2-tailed Student t test was performed to evaluate statistical significance for comparisons between two groups. One-way ANOVA was performed for the comparisons between three or more groups. Dunnett's test was used to account for multiple comparisons. Linear regression analysis was performed for the correlation of CCRL2 RNA levels with the RNA levels of DNMT genes and PRC2 complex genes and P-value was adjusted for multiple comparisons using Bonferroni correction. Univariate linear regression analysis was performed for the correlation of CCRL2 levels with patients' clinicopathological characteristics. Kaplan-Meier analysis was performed for the association of CCRL2 expression with overall survival.



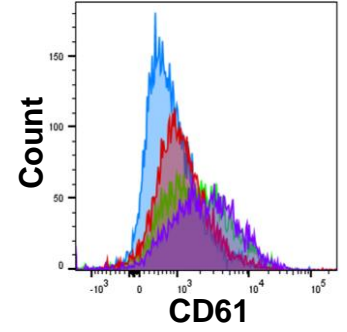
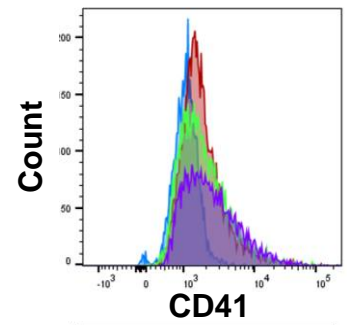
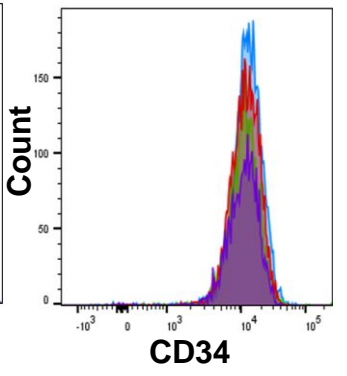
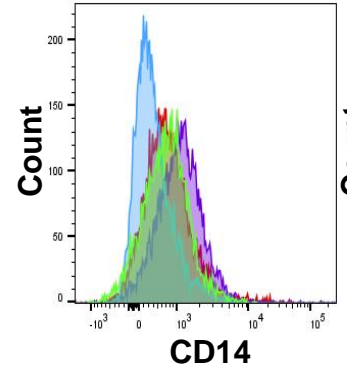
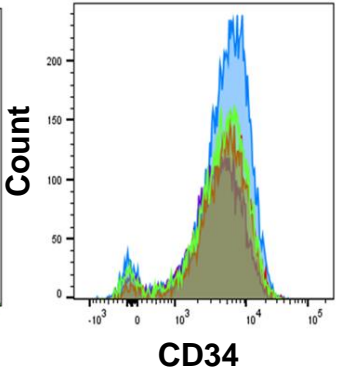
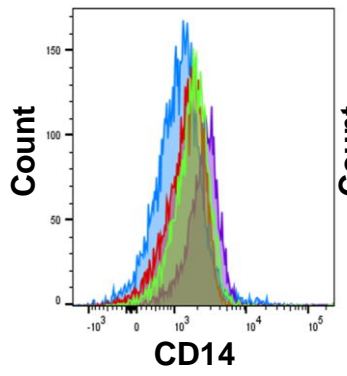
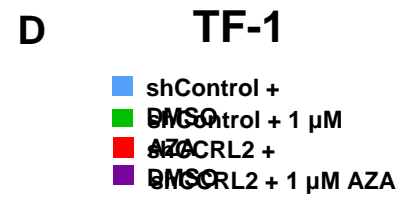
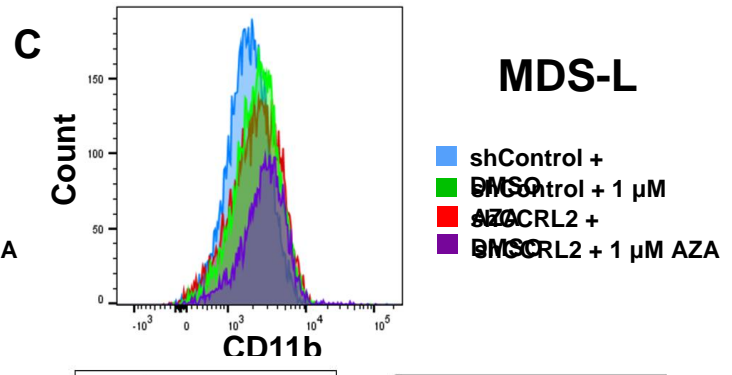
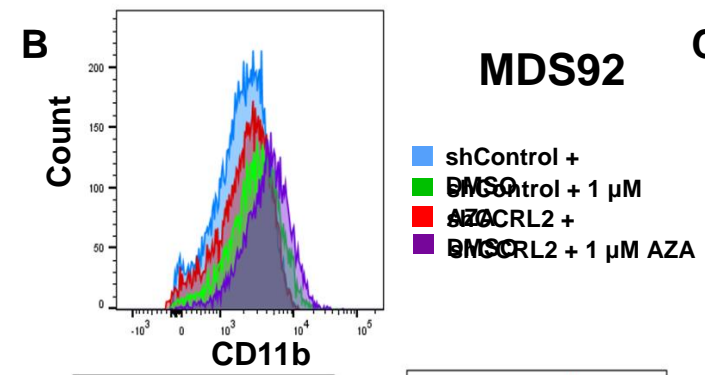
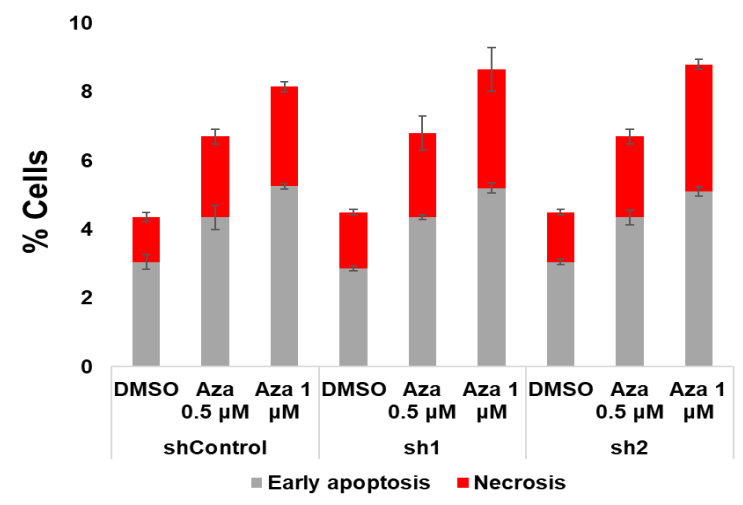
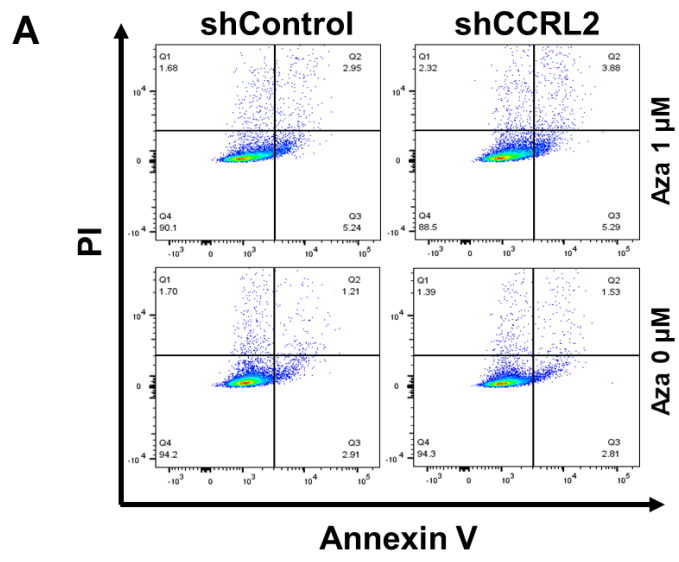


Supplementary Figure 2

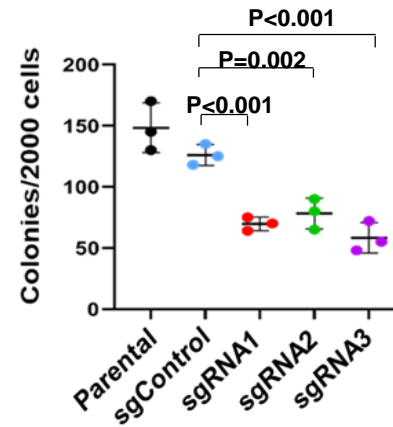
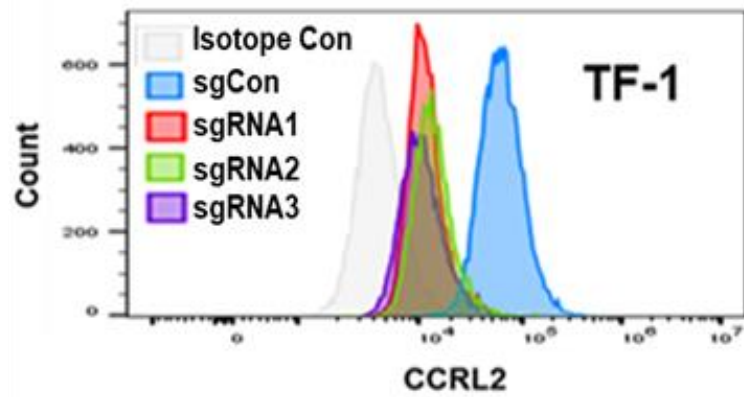
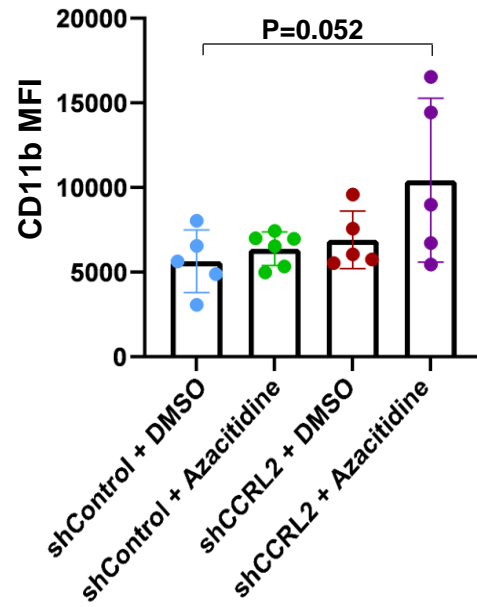
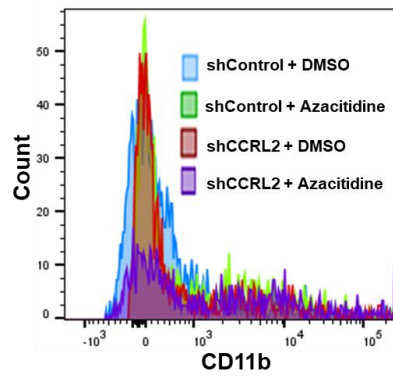
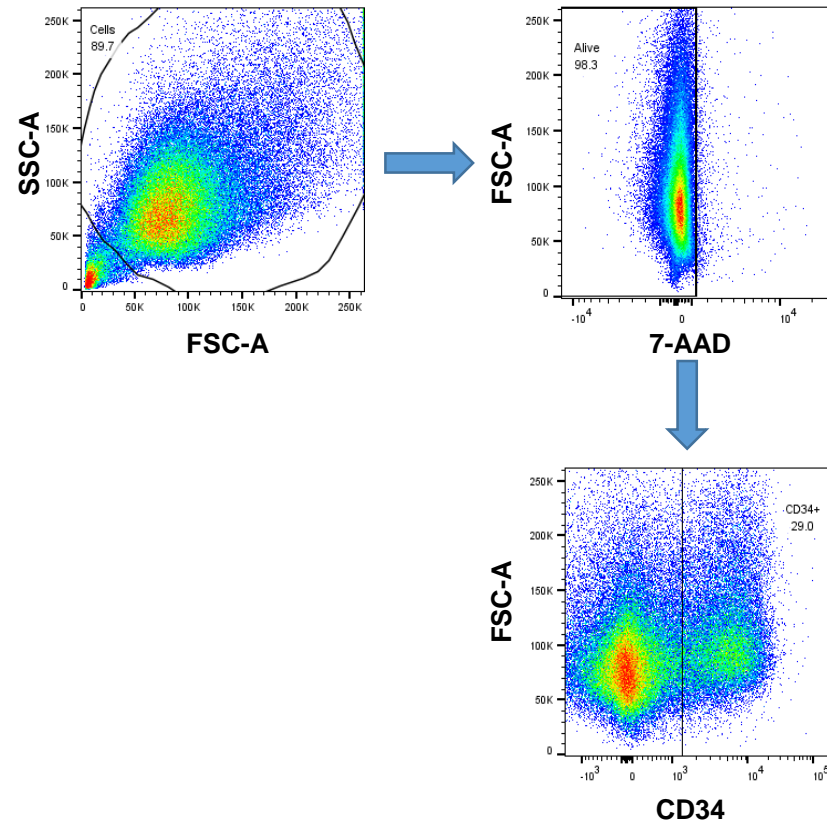




Supplementary Figure 3



Supplementary Figure 4

**A****B****C**

Supplementary Figure 5

## SUPPLEMENTARY FIGURES LEGENDS

**Supplementary Figure 1. A.** Volcano plot of RNA-sequencing data comparing TF-1 cells transduced with shControl and shCCRL2 lentiviruses. **B.** Principal component analysis (PCA) of RNA sequencing data comparing TF-1 cells transduced with shControl and shCCRL2 lentiviruses. **C.** Pathways upregulated in TF-1 cells transduced with shCCRL2 compared to TF-1 cells transduced with shControl identified with GSEA.

**Supplementary Figure 2.** Correlation of CCRL2 and DNMT or PRC2 complex component RNA expression based on RNA-sequencing data from 228 MDS samples derived from the BloodSpot database (GSE42519, GSE13159, GSE15434, GSE61804, GSE14468, and TCGA).

**Supplementary Figure 3. A.** CCRL2 knockdown by two different lentiviruses (sh1 and sh2) increased the inhibitory effect of 0.25 (P=0.005 with sh1 and P=0.022 with sh2), 0.5 (P=0.007 with sh1 and P=0.005 with sh2) and 1  $\mu$ M azacitidine (P=0.005 with sh1 and P=0.004 with sh2) in the clonogenicity of MDS92 cells, n=3. **B.** CCRL2 knockdown by two different lentiviruses (sh1 and sh2) increased the inhibitory effect of 0.25 (P=0.013 with sh1 and P=0.035 with sh2), 0.5 (P=0.005 with sh1 and P=0.110 with sh2) and 1  $\mu$ M azacitidine (P=0.005 with sh1 and P=0.009 with sh2) in the clonogenicity of MDS-L cells, n=3. **C.** CCRL2 knockdown by two different lentiviruses (sh1 and sh2) increased the inhibitory effect of 0.1 (P=0.053 with sh1 and P=0.032 with sh2), 0.25 (P=0.027 with sh1 and P=0.037 with sh2), 0.5 (P=0.004 with sh1 and P=0.006 with sh2) and 1  $\mu$ M azacitidine (P=0.001 with sh1 and sh2) in the clonogenicity of TF-1 cells, n=3. **D.** Serial passage of MDS-L cells in methylcellulose medium showed that CCRL2 KD and azacitidine overall induced the decrease of the relative number of colonies from passage 1 to passage 3. **E.** Serial passage of TF-1 cells in methylcellulose medium showed that CCRL2 KD induced the decrease of the relative number of colonies from passage 1 to passage 2 (P=0.005). Treatment with

0.5  $\mu\text{M}$  azacitidine induced the decrease of the relative number of colonies from passage 1 to passage 2 ( $P=0.025$ ) and passage 3 ( $P=0.012$ ) and 1  $\mu\text{M}$  azacitidine induced the decrease of the relative number of colonies from passage 2 to passage 3 ( $P<0.001$ ). CCRL2 KD further induced the decrease of the relative number of colonies from passage 1 to passage 2 in TF-1 cells treated with 1  $\mu\text{M}$  azacitidine ( $P=0.006$ ). \*  $P<0.05$ , \*\*  $P<0.01$ .

**Supplementary Figure 4. A.** Impact of CCRL2 KD in the percentage of early apoptotic and necrotic TF-1 cells treated with 0.5 or 1  $\mu\text{M}$  azacitidine. **B.** Representative flow cytometry graphs showing that CCRL2 KD increases the upregulation of CD11b, and CD16 in the surface of MDS92 cells caused by 1  $\mu\text{M}$  azacitidine. **C.** Representative flow cytometry graphs showing that CCRL2 KD increases the upregulation of CD11b, and CD16 in the surface of MDS-L cells caused by 1  $\mu\text{M}$  azacitidine. **D.** Representative flow cytometry graphs showing that CCRL2 KD increases the upregulation of CD41, and CD61 in the surface of TF-1 cells caused by 1  $\mu\text{M}$  azacitidine.

**Supplementary Figure 5. A.** Cas9 and sgRNAs were delivered to TF-1 cells via electroporation following single cell cloning, various clones were sequenced and the clones with the confirmed CCRL2 alteration were evaluated by flow cytometry. Methylcellulose assay confirmed that CCRL2 deletion suppresses the clonogenicity of TF-1 cells. **B.** CD11b expression in hCD45+ cells from the bone marrow aspirates of NSG mice was assessed by flow cytometry. Mice engrafted with shCCRL2 cells and treated with azacitidine had the highest expression of CD11b. **C.** Representative flow cytometry gating strategy used for the analysis of CCRL2 expression in CD34+ cells from bone marrow aspirates derived from patients with MDS and MDS/MPN.

## **SUPPLEMENTARY TABLES LEGENDS**

**Supplementary Table 1.** Clinicopathological characteristics of MDS and MDS/MPN patients at the time of the sample

**Supplementary Table 2.** Univariate linear regression analysis of patient' clinicopathological characteristics with the CCRL2 protein expression.

**Supplementary Table 3.** Johns Hopkins University NGS panel